Thermally stimulated depolarization current and Mössbauer spectroscopy of iron-doped niobophosphate glasses

C. J. DE OLIVEIRA
Departamento de Física e Química, UECE, Av. Paranjana 1700, (60715) Fortaleza, CE, Brazil

J. A. C. DE PAIVA, P. C. BARBOSA, J. MENDES FILHO, J. C. P. DE OLIVEIRA, A. SERGIO BEZERRA SOMBRA
Departamento de Física, UFC, P.O. Box 6030, (60450) Fortaleza, CE, Brazil

N. ARANHA, L. C. BARBOSA
Instituto de Física, UNICAMP, P.O. Box 6165, (13081) Campinas, SP, Brazil

O. L. ALVES
Instituto de Química, UNICAMP, P.O. Box 6154, (13081) Campinas, SP, Brazil

Niobophosphate glasses (P_2O_5-PbO-Nb_2O_5-K_2O-$X$$Fe_2O_3$), were studied using thermally stimulated depolarization currents and Mössbauer spectroscopy in samples of different iron concentrations, and were subjected to oxidation and reduction processes. The use of both techniques provided new information about the distribution of iron and niobium between tetrahedral and octahedral sites.

1. Introduction
In recent years, glasses containing Nb_2O_5 have been of great interest to scientists owing to their use as a non-linear photonic material [1, 2]. However, unlike silicates and phosphates, very little work has been performed on niobate glasses. Many authors have studied the coordination number of niobium ions in glass networks. Work by Tatsumisago *et al.* [3] has suggested that the niobium atoms have a coordinate number of 6. Rach Kovskaya and Bobkova [4] studied glasses composed of P_2O_5-Nb_2O_5-TiO_2-Fe_2O_3 and P_2O_5-Nb_2O_5-V_2O_5-TiO_2 by infrared spectroscopy. This experimental study indicates the existence of NbO_4 and NbO_6 units. Wang [5] using Raman and EXAFS spectroscopy confirmed that there are both NbO_4 and NbO_6 polyhedra coexisting in a glass network.

A new family of P_2O_5-PbO-Nb_2O_5-K_2O glasses doped with iron was prepared and studied using Mössbauer spectroscopy and thermally stimulated depolarization currents (TSDC). The results of this study, as well as the preparation of this new family of glasses, are reported.

2. Experimental procedure
2.1. Preparation of the glasses
Glasses were made in P_2O_5-PbO-Nb_2O_5-K_2O-$X$$Fe_2O_3$ systems. They were melted in quartz crucibles at 1340 °C for 30 min in an r.f. furnace [15]. The glass composition was 25.04% P_2O_5, 26.25% PbO, 31.91% Nb_2O_5, 16.80% K_2O and X was 0%, 0.5%, 3% and 5% Fe_2O_3. Chemically pure reagents were used as raw materials. Samples thus prepared are referred to here as being in their original preparation state. Oxidation or reduction of the sample was achieved by subsequent heat treatment in air or a pure hydrogen atmosphere for 1 h.

In TSDC experiments, the sample was polarized at a constant temperature $T_0 = 300$ K for a fixed time $t_0 = 1$ h and then rapidly cooled to $T_f \approx 100$ K with the field applied. The field was then removed and the polarization current recorded as the sample being heated to a complete discharge. All samples were plates of 0.25 cm^2 × 1 mm. The discharge current was recorded with a Keithley electrometer.

2.2. Mössbauer spectroscopy
The Mössbauer effect measurements were carried out at room temperature with a Driver–Transducer–MWE (MR 250), a Function Generator ELSCINT (MFG-3A), a Multichanel ORTEC (6240 B) and an analyser ELSCINT (SCA-N-3). The X-ray source, ^{57}Co, was doped with palladium (New England Nuclear) at room temperature. A proportional counter (Reuter Stokes), was used as the detector for the γ-ray. The measured samples, either in the original state or after being heat treated, were in powdered form.

2.3. Thermally stimulated depolarization current (TSDC)
The TSDC method has recently been used to investigate alkali motion in glasses [6–8]. With this technique

a sample is polarized by an applied field, E_0, for a time t_0, at a given polarization temperature, T_0. This polarization is frozen in by lowering the temperature of the sample to T_f. With the field removed, the sample is heated at a constant rate $b = dT/dt$. The relaxation of any polarization is detected as an induced current.

Most alkali silicate glasses [6] showed two TSDC peaks, and a high-temperature background (HTB) was also found [9]. TSDC peaks and HTB were associated with alkali ion motion, the latter being due to translational alkali ion motion responsible for d.c. conductivity [10].

Polarization caused by the d.c. conduction of the alkaline ion [9] or orientational polarization of alkaline non-bridging oxygens (NBO) gives the same theoretical results for the relaxation. In the Appendix we give the theoretical details of the TSDC. Theoretical predictions for TSDC, were obtained from numerical solution of Equations A3–A5 in the Appendix.

2.4. Dielectric function measurement
The samples used were plates of $10 \times 10 \times 1$ mm^3. The dielectric measurements were made with a capacitance bridge (General Radio model 1615-A) in conjunction with a lock-in amplitier (EG & G model 5208). This system allowed frequency measurements in the range 5 Hz–100 kHz.

3. Results and discussion
Fig. 1a shows a typical Mössbauer spectrum for the 5% iron-doped sample in the original preparation state. The existence of Fe^{2+} and Fe^{3+} ions is clear in this spectrum. Assuming that Fe^{2+} and Fe^{3+} ions have different kinds of coordination, the spectra were fitted with four pairs of lorentzian curves.

The Fe^{3+} ions with a greater value of quadrupole splitting, QS, are supposed to be in tetrahedral coordination, while the Fe^{2+} ions with greater value of QS are supposed to be in octahedral coordination, and the small value of QS is associated with tetrahedral coordination [14].

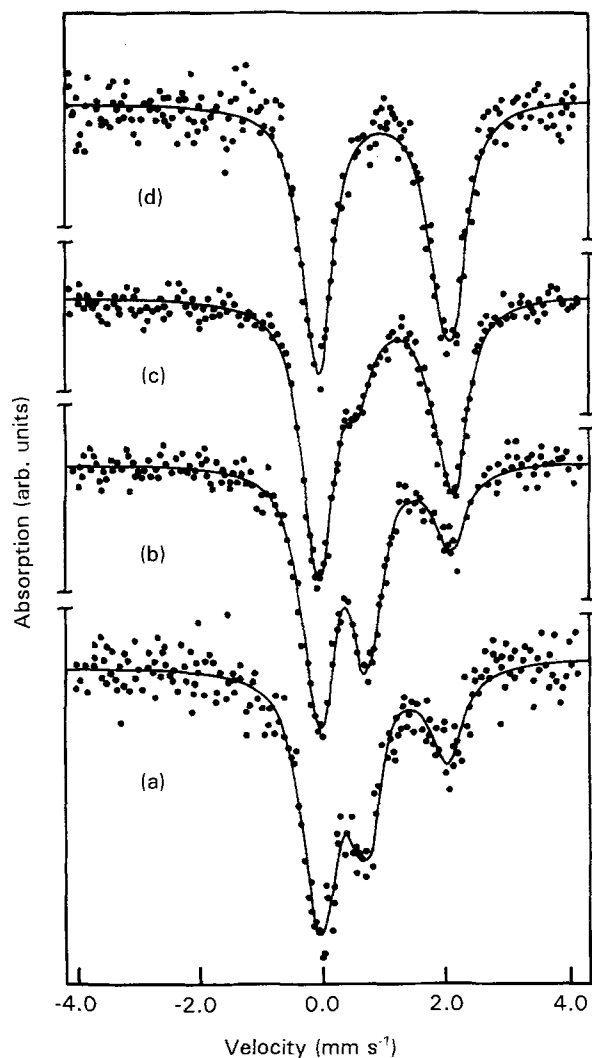According to the fitting (Table I), the sample in the original state presents the Fe^{3+} ion in tetrahedral and

Figure 1 Doped sample ($x = 5\%$) (a) without heat treatment, (b) with heat treatment (H_2) reduction at 200 °C, (c) with heat treatment (H_2) reduction at 400 °C, (d) with heat treatment (H_2) reduction at 600 °C.
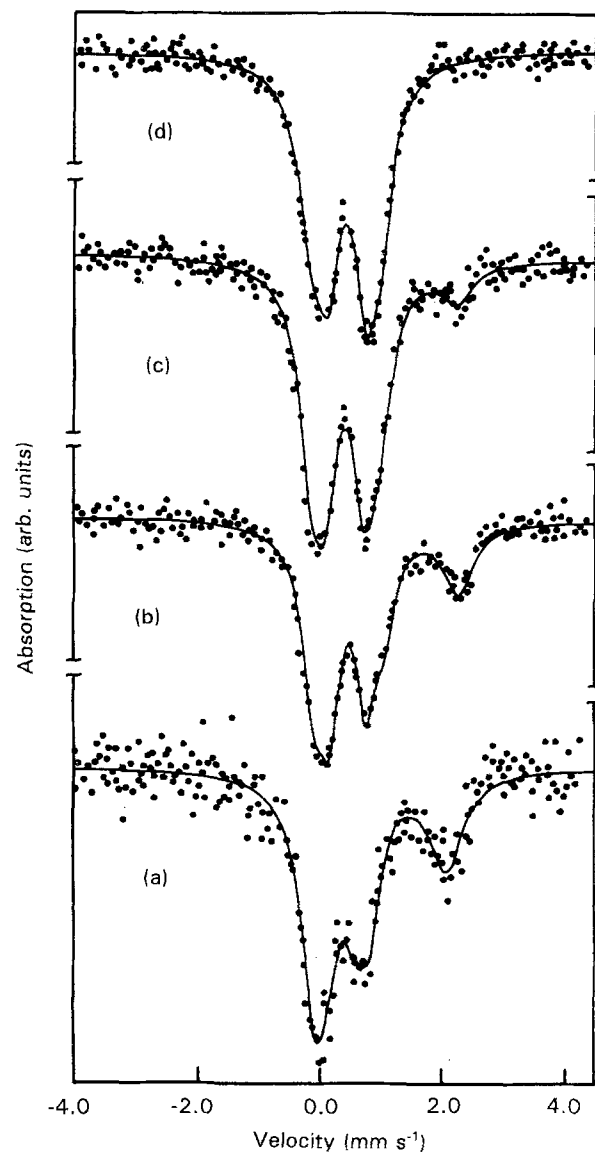

Figure 2 Doped sample ($x = 5\%$) (a) without heat treatment, (b) with heat treatment (O_2) oxidation at 200 °C, (c) with heat treatment (O_2) oxidation at 400 °C, (d) with heat treatment (O_2) oxidation at 600 °C.

TABLE I Mössbauer parameters for iron niobophosphate glasses $X = 5\%$

	Temperature (°C)	Iron III Tetrahedral				Iron III Octahedral				Iron II Octahedral				Iron II Tetrahedral			
		δ_1^a (mm s⁻¹)	Δ_1^b (mm s⁻¹)	τ_1^c (mm s⁻¹)	A_1^d (%)	δ_2^a (mm s⁻¹)	Δ_2^b (mm s⁻¹)	τ_2^c (mm s⁻¹)	A_2^d (%)	δ_3^a (mm s⁻¹)	Δ_3^b (mm s⁻¹)	τ_3^c (mm s⁻¹)	A_3^d (%)	δ_4^a (mm s⁻¹)	Δ_4^b (mm s⁻¹)	τ_4^c (mm s⁻¹)	A_4^d (%)
Original state		0.38	0.92	0.45	32.76	0.38	0.44	0.45	27.19	0.99	2.18	0.65	40.05				
Oxidation	200	0.42	1.12	0.39	23.62	0.39	0.58	0.39	45.93	0.98	2.32	0.58	30.46				
	400	0.36	1.07	0.45	37.60	0.36	0.60	0.45	49.03	0.92	2.45	0.58	13.37				
	600	0.34	1.06	0.53	59.06	0.36	0.56	0.42	40.94								
Reduction	200	0.41	0.95	0.39	29.79	0.39	0.53	0.39	35.97	0.96	2.31	0.58	34.24				
	400					0.41	0.51	0.52	24.94	1.06	2.24	0.52	56.12	0.97	1.88	0.52	18.94
	600									1.12	2.25	0.52	55.49	1.07	1.90	0.52	44.51
Oxidation–reduction	600									1.09	2.24	0.52	21.53	1.07	1.73	0.52	78.47
Reduction–oxidation	600	0.34	1.06	0.39	47.73	0.36	0.45	0.39	52.27								

ᵃ δ, isomer shift.
ᵇ Δ, quadrupole splitting
ᶜ τ, linewidth
ᵈ A, Area.

octahedral coordination with QS = 0.92 and 0.44 mm s⁻¹.

The Fe^{2+} ion is in octahedral coordination with QS = 2.18 mm s⁻¹. If the sample was further treated by a reduction process, the Fe^{2+} band started increasing and Fe^{3+} decreasing (see Table I and Fig. 1). The final state was reached when the Fe^{2+} ion occupied two coordinations, with QS = 2.25 and 1.9 mm s⁻¹.

In the case when the sample was treated by an oxidation process we observed the inverse effect. The Fe^{3+} resonance started increasing up to 100% and the final state contained two coordination states with QS = 1.06 and 0.56 mm s⁻¹ (see Fig. 2 and Table I).

The above results indicate a very efficient conversion of $Fe^{3+} \rightleftharpoons Fe^{2+}$. The reduction process in these glasses was achieved by annealing the sample in atmospheres with low oxygen pressure

$$2\,Fe^{3+} + O^{2-} \rightarrow 2\,Fe^{2+} + 1/2\,O_2 \qquad (1)$$
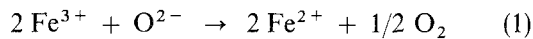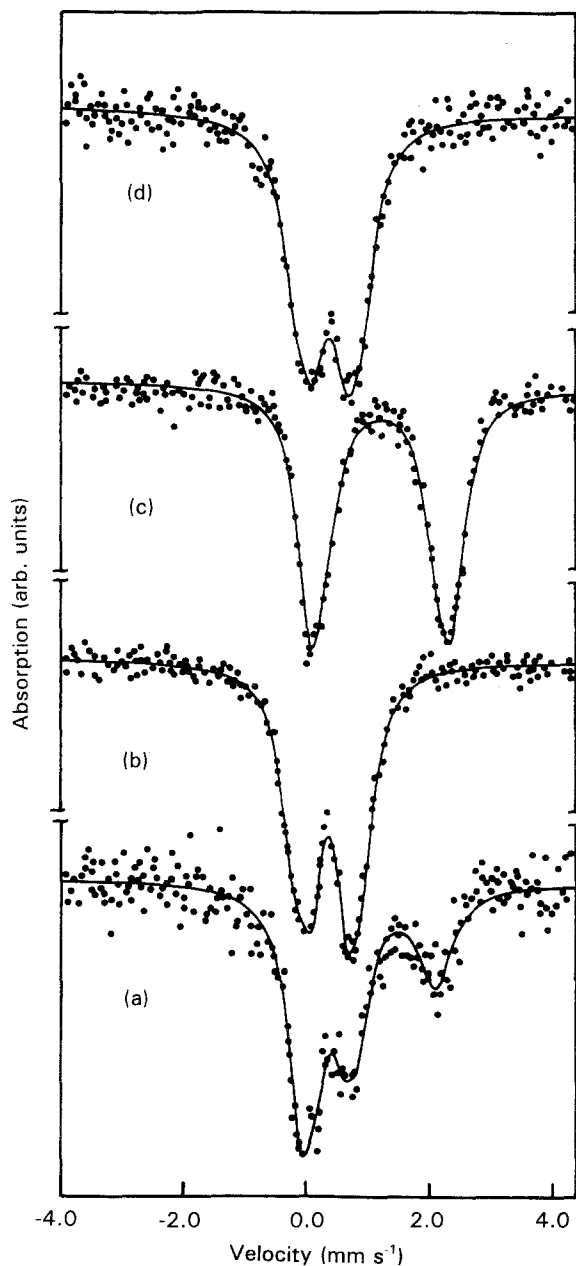
In Fig. 3 the efficiency of the process can be observed.

Figure 3 Doped sample ($x = 5\%$) (a) without heat treatment, (b) oxidation at 600 °C, (c) oxidation at 600 °C followed by reduction at 600 °C, (d) reduction at 600 °C followed by oxidation at 600 °C.

An original sample (Curve a) was submitted to an oxidation process at 600 °C (Curve b) followed by a reduction process at 600 °C (Curve c), and to a further oxidation process (Curve d) (see also Table I).

The site symmetry occupied by Fe^{3+} and Fe^{2+} in niobium compounds is a very much discussed subject in the literature. It is well accepted that the Fe^{3+} ion replaces a Nb^{5+} ion in the NbO_6 octahedra [4, 11].

Owing to the charge difference, O^{2-} vacancies are produced; however, in the case of Fe^{2+}, the situation is more uncertain. It was observed that the heat treatment in the powdered sample was much more effective than sample plates. The Mössbauer spectra, of a sample in a plate geometry submitted to an oxidation process at 600 °C is similar to Fig. 2c. Assuming that the relaxation process is associated with a dipole potassium vacancy, the effect of iron doping in the resonance process is as presented in Fig. 4. All the samples were in the original state with increasing amounts of iron.

From Fig. 4 and Table II we can conclude that the activation energy, E, decreases with increasing iron doping. This effect is associated with the increase of vacancy numbers and, at the same time, increases with decreasing dipolar distance. These effects lead to a decrease in activation energy and peak temperature, T_p, of the depolarization current (Equation A4).
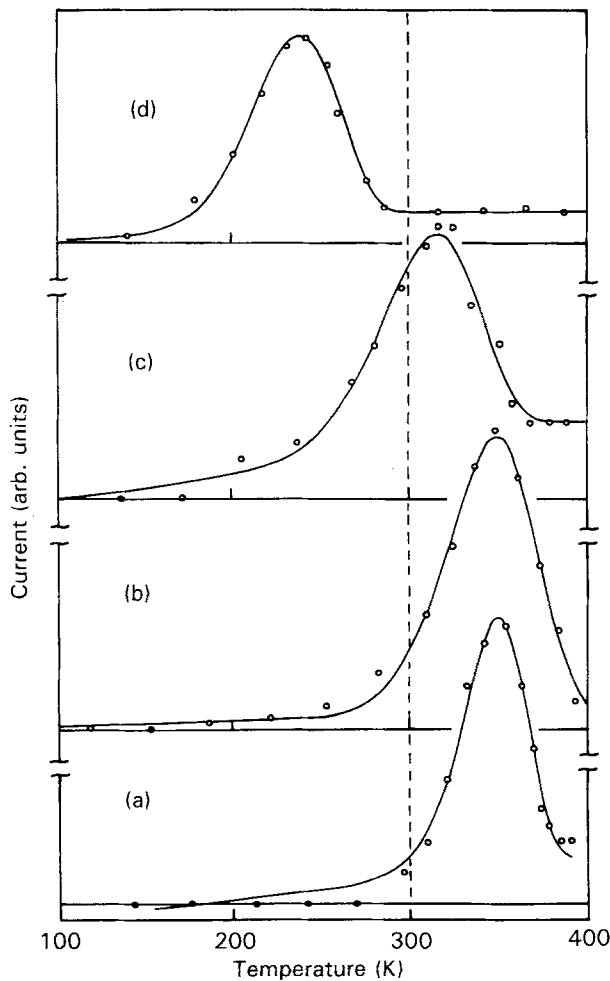
In order to investigate the effect to Fe^{2+} and Fe^{3+} ions, doped and undoped samples were subjected to a process of oxidation and/or reduction. Fig. 5a shows the depolarization resonance for an undoped sample subjected to 800 V in its original state. After a reduction treatment there was a decrease in the peak temperature (Table III) of 33 K (Fig. 5b); after oxidation treatment, T_p increases again. This decrease in T_p after the reduction process could be associated with the reduction of the niobium $Nb^{5+} \rightarrow Nb^{3+}$ which creates vacancies. According to the Mössbauer results, the Fe^{2+} and Fe^{3+} ions in the reduced and oxidized samples, were in tetrahedral and octahedral co-ordination states. Looking now at Fig. 6 and Table III, we can infer that the inhomogeneous relaxation process in reduced samples is much more effective compared to oxidized samples. After the reduction process (Fig. 6b and Table III) the relaxation time increases from 1.49×10^{-3} s to 2.14 s, and decreases to 4.3×10^{-3} s after oxidation. This is a clear indication that the Fe^{2+} ions are in a more spread site distribution compared to Fe^{3+} ions.

TABLE II TSDC parameters without heat treatment, $V = 800$ V

X (%)	T_p (K)	E (eV)	τ_p (s)	ΔT (K)
0.0	335	0.54	3.0×10^{-6}	
0.5	343	0.38	4.1×10^{-4}	12
3.0	313	0.27	1.0×10^{-2}	42
5.0	233	0.16	6.4×10^{-2}	122

Figure 4 TSDC: (a) $X = 0\%$, without heat treatment, $V = 800$ V; (b) $X = 0.5\%$, without heat treatment, $V = 800$ V; (c) $X = 3\%$, without heat treatment, $V = 800$ V; (d) $X = 5\%$, without heat treatment, $V = 800$ V.
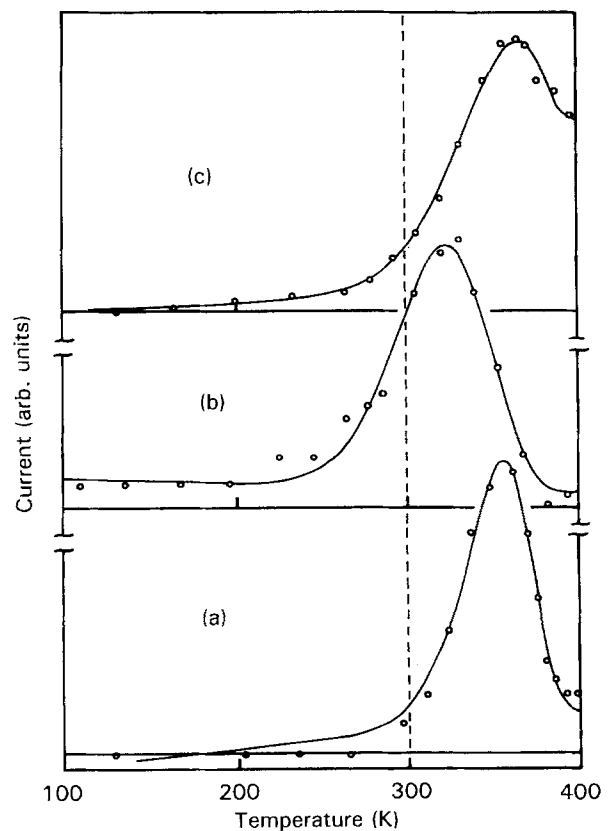

Figure 5 TSDC: (a) $X = 0\%$, without heat treatment, $V = 800$ V; (b) $X = 0\%$, reduced at 600 °C, $V = 800$ V; (c) $X = 0\%$, reduction followed by oxidation at 600 °C, $V = 800$ V.

TABLE III TSDC parameters for niobophosphate glasses with heat treatment

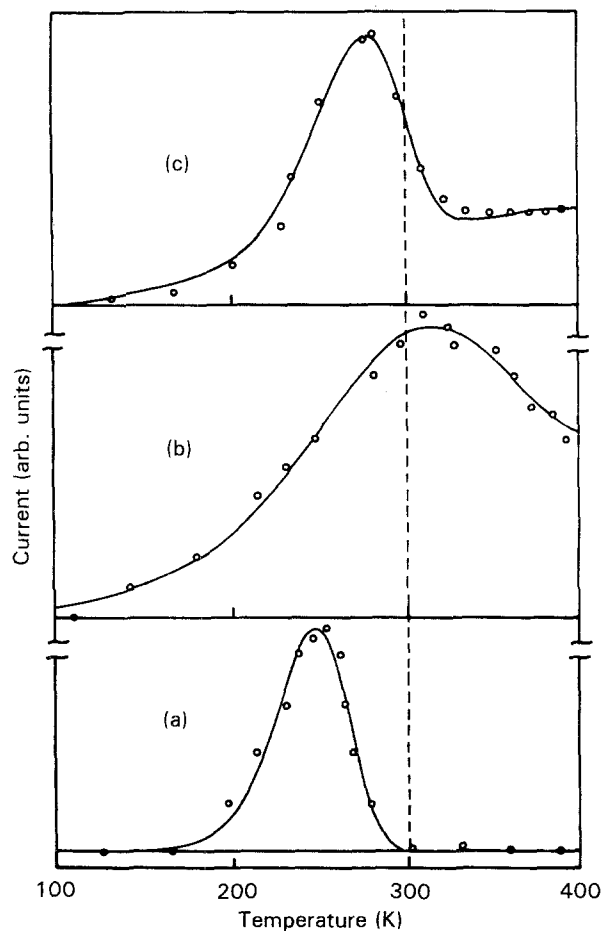| $X(\%)$	V (V)	Original state		Reduced	ΔT (K)	Oxidized	ΔT (K)
0	400	T_p (K)	357	334	23	359	-2
		E (eV)	0.63	0.35		0.28	
		τ (s)	1.7×10^{-7}	1.2×10^{-3}		3.1×10^{-2}	
		$a\,(10^{-13}\,\text{A})$	16	9.94		38.6	
	800	T_p (K)	355	322	33	363	-8
		E (eV)	0.54	0.31		0.35	
		τ (s)	3.10×10^{-6}	3×10^{-3}		2.6×10^{-3}	
		$a\,(10^{-13}\,\text{A})$	8.23	9.76		47.1	
	1200	T_p (K)	348	342	6	358	-10
		E (eV)	0.42	0.46		0.26	
		τ (s)	2×10^{-4}	3×10^{-5}		6.7×10^{-2}	
		$a\,(10^{-13}\,\text{A})$	8.75	5.04		13.36	
5	400	T_p (K)	253	297	-44	277	-24
		E (eV)	0.25	0.14		0.25	
		τ (s)	1.49×10^{-3}	2.14		4.3×10^{-3}	
		$a^a\,(10^{-13}\,\text{A})$	4.49	6.23		30.3	
	800	T_p (K)	233	312	-79	279	-46
		E (eV)	0.16	0.14		0.25	
		τ (s)	6.4×10^{-2}	2.62		5.6×10^{-3}	
		$a^a\,(10^{-13}\,\text{A})$	27.5	7.34		54.9	
	1200	T_p (K)	258	338	-80	282	-24
		E (eV)	0.25	0.16		0.29	
		τ (s)	1.5×10^{-3}	1.64		9.7×10^{-4}	
		$a^a\,(10^{-13}\,\text{A})$	4.8	4.84		10.5	

$^a a$, maximum applitude.

Figure 6 TSDC: (a) $X = 5\%$, without heat treatment, $V = 400$ V; (b) $X = 5\%$, reduced at 600 °C, $V = 400$ V; (c) $X = 5\%$, reduction followed by oxidation at 600 °C, $V = 400$ V.

The Mössbauer parameters are such that, on average, the linewidths, τ_{oct} and τ_{tet}, of Fe^{2+} ions are bigger compared with those of Fe^{3+} ions for the same heat treatment sequences in Table I which agree with the TSDC results.

Subjecting an iron-doped sample (5%; Fig. 6a), in the original state to a reduction treatment (Fig. 6b), there was a decrease of E, in accordance with the increase in the number of vacancies associated with the presence of Fe^{2+} in the niobium sites. In this case, the relaxation time increased by three orders of magnitude on average, as expected. After the oxidation process the activation energy increased again. This behaviour should be associated with the decrease in the number of vacancies for Fe^{3+} compared to Fe^{2+}.
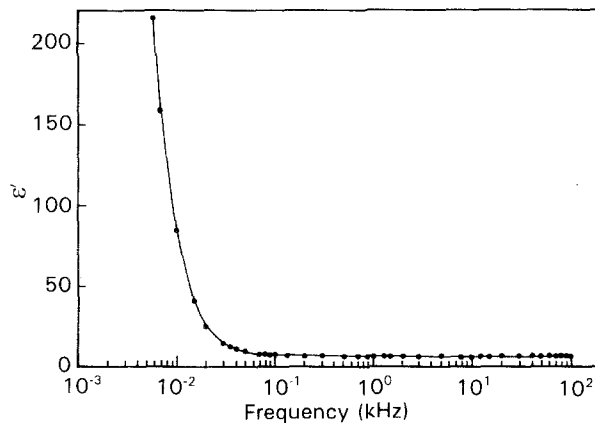

Figure 7 Real dielectric function for $X = 5\%$, without heat treatment.

One interesting feature of the present results is that the maximum temperature, T_p, and the peak intensity of the TSDC signal are dependent on the polarizing voltage. This effect has already been reported by other authors [12, 13] and is probably associated with interface charges in inhomogeneous dielectrics due to the Maxwell Wagner effect [11]. This effect is very pronounced in heterogeneous dielectrics and especially in glasses.

Fig. 7 shows the dielectric function of a glass with $X = 5\%$. The characteristic of the interface polarization is associated with the strong increase of the dielectric function at very low frequencies. In Table III the effect could be found for a sample subjected to the same heat treatment but to different polarizing voltages.

4. Conclusions

Niobophosphate glasses, P_2O_5–PbO–Nb_2O_5–K_2O–XFe_2O_3, were studied using TSDC and Mössbauer spectroscopy. The effect of iron doping was examined under reduction and oxidation conditions. The conversion $Fe^{2+} \rightleftharpoons Fe^{3+}$ and associated vacancies make a very large contribution to the activation energy of the process. The local symmetry of iron and niobium were also investigated.

Acknowledgements

Appendix

The sample properties are determined by C_1, C_2 and R, where C_1 and R are the sample capacitance and resistance, and C_2 is the capacitance, (Fig. A1), between the metal plate electrode and the sample surface.

$$R = -\frac{d}{\sigma A} \quad (A1)$$

with $\sigma T = \sigma_0 \exp(-E/kT)$, d is the sample thickness, A is the electrode area, E is the activation energy, and T is the temperature.

During the TSDC experiment, time, t, and temperature, T, are varied simultaneously at a linear rate

$$\frac{dT}{dt} = b \quad (A2)$$

The current profile as a function of temperature is

$$I(T) = \frac{C_2}{C_1 + C_2} \frac{VA}{d} \left[\frac{\sigma_0}{T} \exp\left(-\frac{E}{KT} \right) \right]$$

$$\times \exp\left[-\frac{A\sigma_0}{bd(C_1 + C_2)} \int_{T_f}^{T} \frac{1}{T} \right.$$

$$\left. \times \exp\left(-\frac{E}{KT} \right) dT \right] \quad (A3)$$

where T_f is the starting temperature, b is the heating rate, V/d is the polarizing field [11].
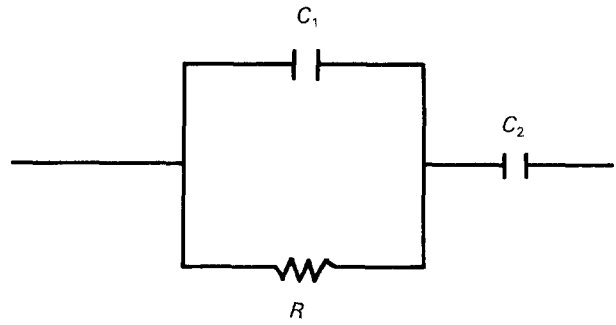

Figure 8 Equivalent circuit representing the sample and interfacial charge on the TSDC experiment.

The peak of the depolarization current at temperature T_p is

$$\frac{E}{KT_p} - 1 = \frac{\sigma_0 A}{bd(C_1 + C_2)} \exp\left(-\frac{E}{KT_p} \right) \quad (A4)$$

From Equation A4, the relaxation time, τ_m, at T_p, given by $R(C_1 + C_2)$, is

$$\tau_m = \frac{T_p}{b} \left(\frac{E}{KT_p - 1} \right) \quad (A5)$$

References

1. E. M. VOGEL, *J. Am. Ceram. Soc.* **72** (1989) 719.
2. E. M. VOGEL, S. G. KOSINSKI, D. M. KROL, J. L. JACKEL, S. R. FRIBERG, M. K. OLIVER and J. D. POWERS, *J. Non-Cryst. Solids* **107** (1989) 244.
3. M. TATSUMISAGO, A. HAMADA, T. MINAMI and M. TANAKA, *J. Am. Ceram. Soc.* **66** (1983) 117.
4. G. E. RACH KOVSKAYA and N. M. BOBKOVA, *J. Non-Cryst. Solids* **90** (1987) 617.
5. G. HUANXIU, W. THONGEAI and W. SHIZHUO, *ibid.* **112** (1989) 332.
6. C. M. HONG and D. E. DAY, *J. Mater. Sci.* **14** (1979) 2493.
7. A. DOI, *J. Appl. Phys.* **50** (1979) 1291.
8. W. K. LEE, S. ARONSON-UNGER and A. S. NOWICK, *J. Non-Cryst. Solids* **122** (1990) 197.
9. A. DOI and D. E. DAY, *J. Appl. Phys.* **52** (1981) 3433.
10. B. DUTTA and D. E. DAY, *J. Non-Cryst. Solids* **48** (1982) 345.
11. J. VANDERCHUEREN and J. GSIOT, in "Thermally Stimulated Relaxation in Solids", edited by P. Braunlich (Springer, Berlin, 1979) Ch. 4.
12. W. REUNE, S. K. DATE, J. DEZZI and U. GONSER, *J. Appl. Phys.* **46** (1975) 3914.
13. A. H. BHUIYAN and S. AHMED, *J. Non-Cryst. Solids* **43** (1981) 353.
14. A. MONTENERO, M. FRIGGERI, D. C. GIORI, N. BELKHIRIA and L.D. PYE, *ibid.* **84** (1986) 45.
15. C. J. DE OLIVEIRA, P. C. BARBOSA, J. A. C. DE PAIVA, J. C. P. DE OLIVEIRA, J. MENDES FILHO, N. ARANHA, L. C. BARBOSA, O. L. ALVES and A. S. B. SOMBRA, "Proceedings of the XVI, International Congress on Glass", Madrid, Spain (1992).